


## Bloch oscillations in the spin- $\frac{1}{2}$ XXZ chain

Yankang Liu, Yohei Fuji , and Haruki Watanabe 

*Department of Applied Physics, University of Tokyo, Tokyo 113-8656, Japan*

 (Received 24 June 2021; revised 4 October 2021; accepted 1 November 2021; published 15 November 2021)

Under a perfect periodic potential, the electric current density induced by a constant electric field may exhibit nontrivial oscillations, so-called Bloch oscillations, with an amplitude that remains nonzero in the large system size limit. Such oscillations have been well studied for nearly noninteracting particles and observed in experiments. In this work we revisit Bloch oscillations in strongly interacting systems. By analyzing the spin- $\frac{1}{2}$  XXZ chain, we demonstrate that the current density at special values of the anisotropy parameter  $\Delta = -\cos(\pi/p)$  ( $p = 3, 4, 5, \dots$ ) in the ferromagnetic gapless regime behaves qualitatively the same as in the noninteracting case ( $\Delta = 0$ ) even in the weak electric field limit. When  $\Delta$  deviates from these values, the amplitude of the oscillation under a weak electric field is suppressed by a factor of the system size. We estimate the strength of the electric field required to observe such a behavior using the Landau-Zener formula.

DOI: [10.1103/PhysRevB.104.205115](https://doi.org/10.1103/PhysRevB.104.205115)

### I. INTRODUCTION

Imagine a system of electrons in a one-dimensional (1D) ring [Fig. 1(a)]. Suppose that a static and uniform electric field  $E$  is turned on at time  $t = 0$ . When  $E$  is sufficiently weak, the response of the electric current density  $j(t)$  is dominated by the contribution from the Drude weight  $\mathcal{D}_1$  of the linear response theory [1]. In free space, electrons keep accelerated and the induced electric current density increases linearly as a function of time, i.e.,  $j(t) \simeq \mathcal{D}_1 E t$ . In the presence of a disorder-free lattice with the lattice constant  $a$ , on the other hand, noninteracting electrons get accelerated initially but then start to move backward [Fig. 1(b)], forming an oscillatory motion. Such an oscillation is known as a Bloch oscillation and has been observed in semiconductor superlattices [2–5]. The standard understanding of this phenomenon in the band theory is through the substitution of the crystal momentum  $k \rightarrow k + A(t)$  under the gauge field  $A(t) = Et$  [6]. Since the momentum space has a period  $2\pi/a$ , we see the frequency  $aE/(2\pi)$  of the Bloch oscillation in noninteracting systems. Equivalently, one may understand this periodic dependence of the electric current on  $Et$  as a result of nonlinear responses to higher powers of  $E$  [7].

The adiabatic transport property is known to be strongly affected by interactions and disorders [8,9]. For interacting systems, recent studies revealed that the Drude weight  $\mathcal{D}_N$  ( $N \geq 2$ ) of nonlinear responses tends to diverge in the limit of large system size [7,10,11]. Similar divergence has been observed in noninteracting systems in the presence of a localized impurity [12]. These results imply that the Bloch oscillations in noninteracting and imperfection-free systems may completely disappear when interactions or disorders are added. This is indeed the case for a tight-binding model with a single defect in the limit of the weak electric field [12].

In this work we study the current response of disorder-free interacting electrons at zero temperature. By analyzing the spin- $\frac{1}{2}$  XXZ chain, which can be mapped to a model of spinless electrons interacting with each other between neighboring sites, we find that interacting systems can exhibit Bloch oscillations for fine-tuned values of the interaction  $\Delta = -\cos(\pi/p)$  ( $p = 3, 4, 5, \dots$ ). The frequency of the oscillation in the limit of weak electric field is modified to  $a(p-1)E/(2\pi)$  by interaction ( $p=2$  corresponds to the noninteracting case  $\Delta=0$ ). When  $\Delta$  is not exactly at these special values, the interaction induces level repulsions to the many-body energy levels as a function of the gauge field  $A$ . As a result, the behavior of  $j(t)$  becomes qualitatively different—it still oscillates as a function of  $t$  but with an amplitude inversely proportional to the system size. At the same time, the frequency becomes  $LE/(4\pi)$  and is proportional to the system size. Such behaviors can be seen only when the electric field  $E$  is sufficiently weak, and we give an estimate of the required strength of  $E$  using the Landau-Zener formula [13–15]. Our study is complementary to the previous work [16] which discussed a different electric field regime for the infinite system by the generalized hydrodynamics method.

### II. THE XXZ MODEL

#### A. Definitions

In this work we discuss the spin- $\frac{1}{2}$  XXZ chain

$$\hat{H}(A) = J \sum_{i=1}^L \left( \frac{1}{2} \hat{s}_{i+1}^+ e^{-iA} \hat{s}_i^- + \text{H.c.} + \Delta \hat{s}_{i+1}^z \hat{s}_i^z \right), \quad (1)$$

where  $\hat{s}_i^\alpha$  ( $\alpha = x, y, z$ ) is the spin- $\frac{1}{2}$  operator defined on the site  $i$  and  $\hat{s}_i^\pm = \hat{s}_i^x \pm i\hat{s}_i^y$ ,  $L$  is the system size,  $J$  is the antiferromagnetic coupling constant,  $\Delta$  is the anisotropy parameter, and  $A$  is the vector potential (with the sign convention opposite to the conventional one) associated with the spin rotation symmetry

\*hwatanabe@g.ecc.u-tokyo.ac.jp

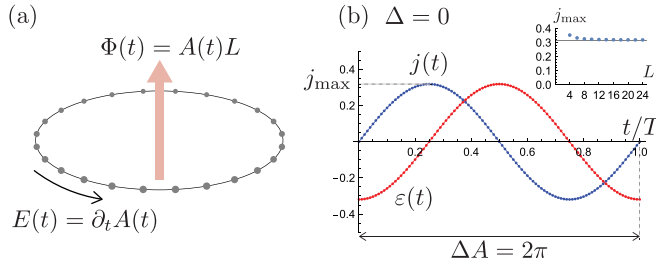


FIG. 1. (a) One-dimensional ring pierced by a flux  $\Phi(t) = A(t)L$ , which induces an electric field  $E(t) = \partial_t A(t)$ . (b) Oscillations of the energy density  $\varepsilon(t)$  and the current density  $j(t)$  for the model (1) with  $A = 2\pi t/T$  and  $L = 24$  in the noninteracting case  $\Delta = 0$ . We set  $T = 1$  in this plot but results are identical up to  $T = 10^6$ , the largest period we computed. Both  $j(t)$  and  $\varepsilon(t)$  show a single oscillation over the period  $T$  where  $A$  increases by  $2\pi$ . Solid curves represent the analytic expressions  $\varepsilon(t) = -L^{-1} \cos A(t) / \sin(\pi/L)$  and  $j(t) = L^{-1} \sin A(t) / \sin(\pi/L)$ . The inset shows the amplitude  $j_{\max}$  as a function of  $L$ , suggesting that it is of  $O(1)$  in the large  $L$  limit.

about the  $z$  axis. The lattice constant  $a$  is set to 1. We impose the periodic boundary condition and identify  $\hat{s}_{L+1}^\alpha = \hat{s}_1^\alpha$ . The conserved current density of this model is defined by

$$\hat{j}(A) = \frac{1}{L} \frac{d\hat{H}(A)}{dA}. \quad (2)$$

The spin chain (1) can be mapped to a model of spinless electrons

$$\begin{aligned} \hat{H}(A) = & \sum_{i=1}^L (t_0 \hat{c}_{i+1}^\dagger e^{-iA} \hat{c}_i + \text{H.c.}) \\ & + \sum_{i=1}^L U \left( \hat{n}_{i+1} - \frac{1}{2} \right) \left( \hat{n}_i - \frac{1}{2} \right) \end{aligned} \quad (3)$$

by the Jordan-Wigner transformation [17], where  $t_0 = J/2$  and  $U = J\Delta$ . The spin current density (2) can thus be regarded as the electric current density of spinless electrons. In the following we set  $J = 1$  and focus on the gapless regime  $-1 < \Delta < 1$  at the zero temperature.

### B. Periodicity of the adiabatic ground state

Let us examine the periodicity of the many-body energy levels of  $\hat{H}(A)$  as a function of  $A$ . Obviously we have  $\hat{H}(2\pi) = \hat{H}(0)$ , but  $\Delta A = 2\pi$  is not the smallest period of this model in the following sense. The gauge field  $A$  is related to the flux  $\Phi = AL$  piercing the hole of the 1D ring [Fig. 1(a)], and  $A = 0$  and  $A = 2\pi/L$  give the physically equivalent flux. In fact, they are connected by a unitary transformation, called the large gauge transformation [18]. Therefore, the entire spectrum of  $\hat{H}(A)$  has a period  $\Delta A = 2\pi/L$ . This is the case regardless of the specific choice of  $\Delta$ .

In contrast, the ‘‘adiabatic ground state’’ has a longer period that depends on  $\Delta$  [19]. Let  $|\Psi\rangle$  be the ground state at  $A = 0$ . Among the stroboscopic eigenstates of  $\hat{H}(A)$ , we keep track of the state that is smoothly connected to  $|\Psi\rangle$  as a function of  $A$ . This is what we call the adiabatic ground state  $|\Psi_{\text{AGS}}(A)\rangle$ . See red curves in Fig. 2 for illustration. In the following we

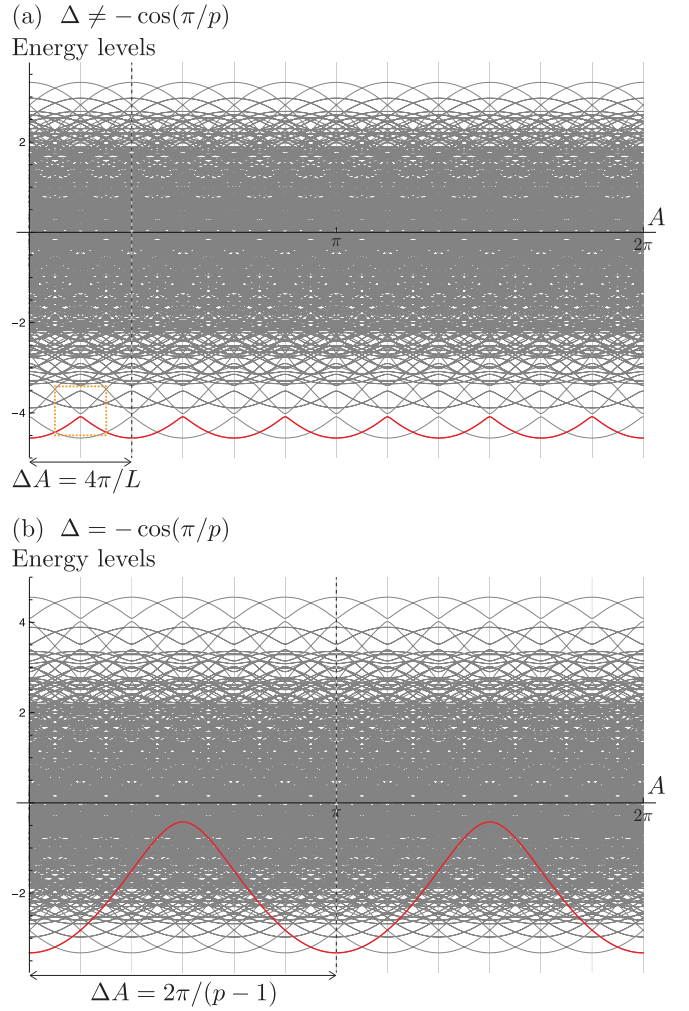


FIG. 2. The many-body energy levels of  $\hat{H}(A)$ , obtained by the exact diagonalization, for  $L = 12$  as a function of the gauge field  $A$  in the case of (a) a generic value  $\Delta = +0.5$  and (b) a special value  $\Delta = -\cos(\pi/3)$  ( $p = 3$ ). Only the states in the  $S_z = 0$  sector are shown. The adiabatic ground state is highlighted with red color. Because  $\Delta \leftrightarrow -\Delta$  corresponds to  $\hat{H}(A) \leftrightarrow -\hat{H}(A)$ , (b) can be seen as the inverted version of (a) in this example.

denote by  $\varepsilon_{\text{AGS}}(A)$  the energy density of the adiabatic ground state.

The flux-threading argument for the Lieb-Schultz-Mattis theorem predicts a level crossing between two levels with distinct momentum eigenvalues 0 and  $\pi$  for translation and time-reversal invariant spin- $\frac{1}{2}$  chains [18]. Hence, the smallest possible value of the period of the adiabatic ground state is  $\Delta A = 4\pi/L$ . This is indeed the case for generic  $\Delta$  [20,21] [Fig. 2(a)]. In particular, the period  $\Delta A$  vanishes in the large  $L$  limit and the energy density  $\varepsilon_{\text{AGS}}(A)$  becomes a constant  $\varepsilon_{\text{AGS}}(0)$  independent of  $A$ .

Exceptions occur at special values of  $\Delta$ , i.e.,  $\Delta = -\cos(\pi/p)$  ( $p = 2, 3, \dots$ ), at which the adiabatic ground state has a much longer period [22].

From numerical investigations we identify the period  $\Delta A = 2\pi/(p-1)$  for  $\Delta = -\cos(\pi/p)$  [23]. This is clearly demonstrated in the left column of Figs. 3(a)–3(c) for the

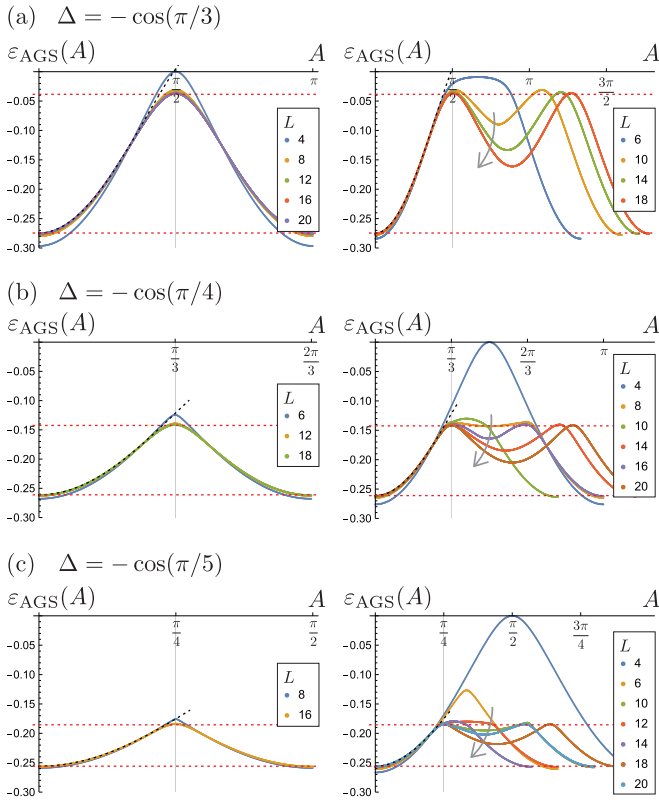


FIG. 3. The energy density of the adiabatic ground state  $\varepsilon_{\text{AGS}}(A)$  as a function of  $A$  for (a)  $\Delta = -\cos(\pi/3) = -0.5$ , (b)  $\Delta = -\cos(\pi/4) = -0.707107$ , and (c)  $\Delta = -\cos(\pi/5) = -0.809017$ . The black dotted curve is the analytic expression for  $L \rightarrow \infty$  up to the  $A^6$  order in (4). The red dotted lines are the analytic expressions for the minimum and the maximum of  $\varepsilon_{\text{AGS}}(A)$  (see the main text).

sequence of the system size  $L = 2(p-1)\ell$  ( $\ell \in \mathbb{N}$ ). For the system size other than  $L = 2(p-1)\ell$ , the apparent period is greater than  $\Delta A = 2\pi/(p-1)$  as long as  $L$  is finite, as shown in the right column of Figs. 3(a)–3(c). However, the dip of the curve  $\varepsilon_{\text{AGS}}(A)$  around  $A = 2\pi/(p-1)$  develops as  $L$  increases (indicated by gray arrows in Fig. 3), and the actual period converges to  $\Delta A = 2\pi/(p-1)$  in the large  $L$  limit. Therefore, the large  $L$  limit of the curve  $\varepsilon_{\text{AGS}}(A)$  is well defined, i.e., does not depend on the sequence of  $L$ . Most importantly, both the period  $\Delta A$  and the amplitude of the oscillation of  $\varepsilon_{\text{AGS}}(A)$  do not vanish in the large  $L$  limit. This difference results in the qualitatively different behaviors of the induced electric current in response to an infinitesimal electric field, as we discuss in the next section.

In Fig. 3 the black dotted curve represents

$$\varepsilon_{\text{AGS}}(A) \simeq \bar{\varepsilon}_{\text{GS}} + \frac{\bar{D}_1}{2!}A^2 + \frac{\bar{D}_3}{4!}A^4 + \frac{\bar{D}_5}{6!}A^6, \quad (4)$$

where  $\bar{\varepsilon}_{\text{GS}}$  is the energy density and  $\bar{D}_n$  is the  $n$ th order Drude weight in the large  $L$  limit. The red dotted lines are the minimum  $\varepsilon_{\text{AGS}}(0) = \bar{\varepsilon}_{\text{GS}}$  and the maximum  $\varepsilon_{\text{AGS}}[\pi/(p-1)]$  of  $\varepsilon_{\text{AGS}}(A)$  in the large  $L$  limit. The analytic expressions of  $\bar{\varepsilon}_{\text{GS}}$  and  $\bar{D}_1$  have long been known [20,24] and the expressions for higher Drude weights  $\bar{D}_3$  and  $\bar{D}_5$  have been obtained in recent studies [7,10]. For the readers' convenience, we include

these expressions in Appendix A. Following the derivation of these quantities, we obtained the analytic expression of the maximum

$$\varepsilon_{\text{AGS}}\left(\frac{\pi}{p-1}\right) = -\frac{1}{4}\cos(\pi/p) + \frac{1}{2}\sin(\pi/p) \times \int_{-\infty}^{\infty} d\omega \frac{\sinh(\pi\omega/p) \tanh(\pi\omega/p)}{\sinh(\pi\omega) \sinh[(p-1)\pi\omega/p]} \quad (5)$$

in the limit of large  $L$ . See Appendix B for the derivation. We see an excellent agreement between our numerics and analytic lines and curves. Assuming that  $\varepsilon_{\text{AGS}}(A)$  converges to a smooth function of  $A$  in the large  $L$  limit, all the nonlinear Drude weights remain finite for the special values of  $\Delta$  [12].

Before closing this section, let us explain how we kept track of the adiabatic ground state  $|\Psi_{\text{AGS}}(A)\rangle$  in our numerical investigation of  $\varepsilon_{\text{AGS}}(A)$ . First, we reduce the number of candidate states by using the spin rotation symmetry about  $z$  axis and the translation symmetry, focusing on the  $S_z = 0$  sector and the momentum  $P = 0$  sector. Next, we discretize  $A \in [0, 2\pi]$  as  $A^{(n)} \equiv n\delta A$  ( $n = 0, 1, 2, \dots$ ). The increment  $\delta A$  needs to be chosen sufficiently small, and in this work we set  $\delta A = \pi/(160L)$ . We start with the unique ground state of  $\hat{H}(A)$  for  $A = A^{(0)} = 0$  and  $A = A^{(1)} = \delta A$ . Then, for  $n > 1$ , we proceed step by step by choosing as  $|\Psi_{\text{AGS}}(A^{(n+1)})\rangle$  the state whose energy density is closest to the linear interpolation

$$\varepsilon_{\text{AGS}}(A^{(n)}) + \delta A[\varepsilon_{\text{AGS}}(A^{(n)}) - \varepsilon_{\text{AGS}}(A^{(n-1)})] \quad (6)$$

among the eigenstates of  $\hat{H}(A^{(n+1)})$  in the  $S_z = P = 0$  sector. We confirm the convergence by changing  $\delta A$ .

### III. TIME EVOLUTION

#### A. Bloch oscillations in the weak field limit

Now, following Refs. [25,26], let us introduce a time dependence to the Hamiltonian (1) by setting  $A = A(t) = 2\pi t/T$  for  $t \geq 0$  and  $A = 0$  for  $t < 0$ . This time-dependent gauge field induces a static and uniform electric field  $E = 2\pi/T$  for  $t \geq 0$ . We assume that the system is in the ground state  $|\Psi\rangle$  of  $\hat{H}(0)$  for  $t < 0$ . The time evolution of the state for  $t \geq 0$  is described by the Schrödinger equation

$$i\frac{d}{dt}|\Psi(t)\rangle = \hat{H}(A(t))|\Psi(t)\rangle. \quad (7)$$

The energy density  $\varepsilon(t)$  and the induced current density  $j(t)$  and at time  $t > 0$  are given by

$$\varepsilon(t) \equiv \frac{1}{L}\langle\Psi(t)|\hat{H}(A(t))|\Psi(t)\rangle, \quad (8)$$

$$j(t) \equiv \langle\Psi(t)|\hat{j}(A(t))|\Psi(t)\rangle = \frac{1}{L}\langle\Psi(t)|\frac{d\hat{H}(A)}{dA}|\Psi(t)\rangle\Big|_{A=A(t)} = \left(\frac{dA(t)}{dt}\right)^{-1}\frac{d\varepsilon(t)}{dt} = \frac{1}{E}\frac{d\varepsilon(t)}{dt}. \quad (9)$$

When  $T$  is sufficiently large for a given  $L$  and  $\Delta$ , the adiabatic theorem [27,28] gives [7]

$$\varepsilon(t) = \varepsilon_{\text{AGS}}(A(t)), \quad (10)$$

$$j(t) = \frac{d\varepsilon_{\text{AGS}}(A)}{dA}\Big|_{A=A(t)}. \quad (11)$$

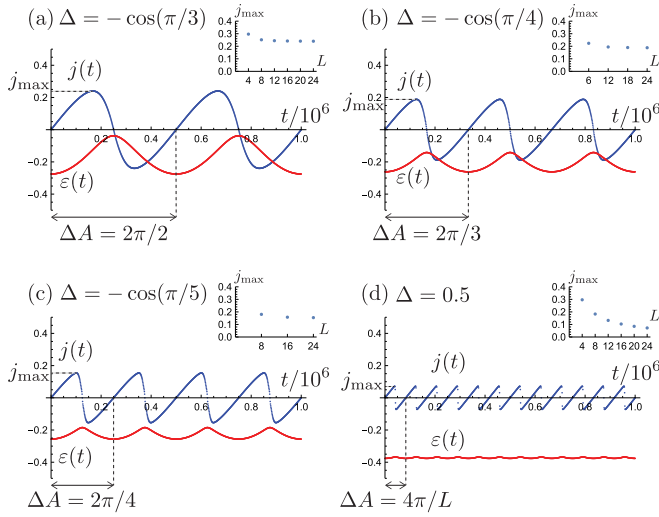


FIG. 4. Oscillations of the energy density  $\varepsilon(t)$  and the current density  $j(t)$  in for (a)  $\Delta = -\cos(\pi/3) = -0.5$ , (b)  $\Delta = -\cos(\pi/4)$ , (c)  $\Delta = -\cos(\pi/5)$ , and (d)  $\Delta = +0.5$ . We set  $L = 24$ ,  $T = 10^6$ , and  $A(t) = 2\pi t/T$  in these calculations. The number of peaks is  $p - 1$  for (a)–(c) and  $L/2$  for (d) as predicted. The inset shows the amplitude  $j_{\max}$  as a function of  $L$ , which remains nonzero in the large  $L$  limit for (a)–(c), while it is inversely proportional to  $L$  and vanishes in the large  $L$  limit for (d).

Namely, the energy density  $\varepsilon(t)$  and the current density  $j(t)$  of the time-dependent problem are fully characterized by the adiabatic ground-state energy density  $\varepsilon_{\text{AGS}}(A)$  of the time-independent system. This immediately implies the possibility of Bloch oscillations even under an infinitesimal electric field for the special values  $\Delta = -\cos(\pi/p)$  ( $p = 2, 3, \dots$ ), where the period  $\Delta A = 2\pi/(p-1)$  of  $\varepsilon_{\text{AGS}}(A)$  remains nonzero in the large  $L$  limit. For the constant electric field described by  $A(t) = Et$ , the temporal period of the oscillation is given by  $\Delta t = \Delta A/E = 2\pi/[(p-1)E]$ , suggesting that the frequency of the Bloch oscillation is  $\nu = (p-1)E/(2\pi)$  for  $\Delta = -\cos(\pi/p)$ .

We demonstrate this prediction by numerically solving the Schrödinger equation using the fourth-order Runge-Kutta method. We set  $dt = 0.001$ . Our results are summarized in Fig. 4. As anticipated, even for  $T = 10^6$ , the amplitudes of the oscillations of the energy density  $\varepsilon(t)$  and the current density  $j(t)$  are of  $O(1)$  for the special values of  $\Delta = -\cos(\pi/p)$  in Figs. 4(a)–4(c). In contrast, they are  $O(L^{-1})$  for the generic case in Fig. 4(d). Over the time period  $T$ , the gauge field  $A(t)$  increases by  $2\pi$  and the number of peaks is  $p - 1$  for the special values in Figs. 4(a)–4(c) and is of  $O(L)$  for the generic case in Fig. 4(d). These are all consistent with the behavior of  $\varepsilon_{\text{AGS}}(A)$  discussed in the previous section. Sharp drops of the electric current  $j(t)$  around  $t = 2\pi(2j - 1)/(LE)$  ( $j = 1, 2, \dots$ ) seen in Fig. 4(d) underlie the divergence of nonlinear Drude weights for generic  $\Delta$ .

### B. Landau-Zener formula for generic $\Delta$

When  $\Delta$  deviates from the special values, the many-body energy spectrum opens a tiny gap  $\Delta E$  between the adiabatic ground state and the next level at  $A = 2\pi/L$ . See the orange

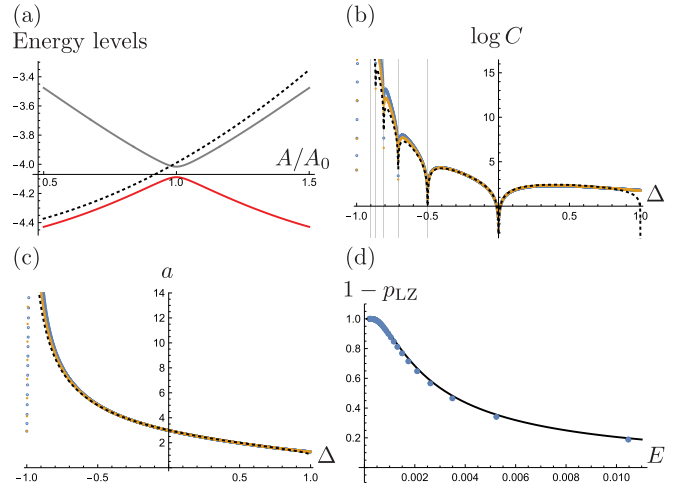


FIG. 5. (a) The zoom-up of the orange dashed box in Fig. 2(a), focusing on the adiabatic ground state and the next level near  $A = A_0 = 2\pi/L$ . The dashed curve represents  $L\varepsilon_{\text{AGS}}(A)$  in the first line of (12). (b) The coefficient  $C$  in (14) obtained by fitting with numerical data. The dotted curve represents the analytic expression in Appendix A. The vertical lines represent  $\Delta = -\cos(\pi/p)$  with  $p = 3, 4, \dots, 7$ . (c) The power  $a$  in (14) obtained by fitting. The dotted curve represents  $a = 4K - 1$ . In (b) and (c) the blue open dots use data for  $L = 12, 14, \dots, 32$  and the yellow filled dots use data for  $L = 20, 22, \dots, 32$  only. (d) Numerical verification of the Landau-Zener formula for  $\Delta = 0.5$  and  $L = 12$ . The blue dots represent  $p_{\text{AGS}}(t)$  in (15) at  $t = 2t_0$  and the solid curve represents  $1 - p_{\text{LZ}}$  given by (13).

dashed box in Fig. 2(a). When  $T$  is large enough, the applied electric field is sufficiently weak and the state  $|\Psi(t)\rangle$  stays in the adiabatic ground state. In contrast, when  $T$  gets smaller, nonadiabatic transition starts to occur. This type of tunneling has been studied for the Hubbard ring of spinful electrons in Refs. [29,30]. Here we estimate the strength of the electric field  $E$  required to avoid nonadiabatic transition in the spin- $1/2$  XXZ chain (1) based on the Landau-Zener formula.

Let us first assume  $\Delta E = 0$ . Then the energy density of the adiabatic ground state around  $A = A_0 \equiv 2\pi/L$  can be approximated, to the leading order of  $L^{-1}$ , by

$$\begin{aligned} \varepsilon_{\text{AGS}}(A) &\simeq \bar{\varepsilon}_{\text{GS}} + \frac{1}{2}\bar{\mathcal{D}}_1 A^2 + O(A^4) \\ &= \bar{\varepsilon}_{\text{GS}} + \frac{1}{2}\bar{\mathcal{D}}_1 A_0^2 + \bar{\mathcal{D}}_1 A_0 (A - A_0) + O[(A - A_0)^2]. \end{aligned} \quad (12)$$

See Fig. 5(a) for comparison with the exact diagonalization for  $L = 12$  and  $\Delta = 0.5$ . The error in the approximation is a finite-size effect. Hence, when  $A(t) = Et$ , the energy difference of the two levels that cross each other at  $A = A_0$  goes as  $\alpha|t - t_0|$  with  $\alpha \equiv 2\bar{\mathcal{D}}_1 A_0 L E = 4\pi\bar{\mathcal{D}}_1 E$  and  $t_0 \equiv A_0/E$ .

When  $\Delta E > 0$ , the Landau-Zener formula [13–15] gives the probability of the nonadiabatic transition

$$p_{\text{LZ}} \equiv \exp\left[-2\pi \frac{(\Delta E/2)^2}{\alpha}\right] = \exp\left[-\frac{(\Delta E)^2}{8\bar{\mathcal{D}}_1 E}\right]. \quad (13)$$

This formula was originally derived for two level systems and  $\Delta E/2$  is identified with the amplitude of the off-diagonal components of the two level Hamiltonian. Here, following

Ref. [29], we apply it to the focused two levels in the many-body spectrum [31].

To make use of the formula (13), we now study the system-size dependence of the finite-size splitting  $\Delta E$ . Here we assume the power-law form [32]

$$\Delta E = CL^{-a}. \quad (14)$$

The leading contribution to  $\Delta E$  comes from the least irrelevant perturbation due to Umklapp scattering [21,33], which gives  $a = 4K - 1 = 2\pi[\arccos(-\Delta)]^{-1} - 1$ , where  $K$  is the Luttinger parameter [34]. We append the analytic expression for  $C$  in Appendix A. For example, we find  $\Delta E \simeq 2\sqrt{3}\pi L^{-2}$  for  $\Delta = 0.5$ . We confirm these analytic expressions by fitting with numerical data up to  $L = 32$ . As shown in Figs. 5(b) and 5(c), we find a good agreement.

Finally, let us verify the Landau-Zener formula (13). We compute the probability of adiabatic process in two ways: one by  $1 - p_{LZ}$  using the last expression of (13) and the other by the overlap

$$p_{\text{AGS}}(t) \equiv |\langle \Psi_{\text{AGS}}(A(t)) | \Psi(t) \rangle|^2 \quad (15)$$

at  $t = 2t_0$ , by numerically solving the time-dependent Schrödinger Eq. (7). For the gap  $\Delta E \simeq CL^{-a}$ , we use the analytic expressions of  $C$  and  $a$ . As shown in Fig. 5(d) for  $\Delta = 0.5$  and  $L = 12$ , they agree unexpectedly well.

These results suggest that, in order to avoid nonadiabatic transition, the electric field must satisfy

$$E \ll \frac{(\Delta E)^2}{8\bar{D}_1} = \frac{C^2}{8\bar{D}_1} L^{-2a}. \quad (16)$$

The right-hand side becomes small quickly as  $L$  increases, suggesting that  $E$  must be chosen very small. In other words, when  $E = 2\pi/T$ , the time interval  $T$  must be chosen quite long. Therefore, it is actually nearly impossible to achieve the adiabatic limit such as the one in Fig. 4(d) in a thermodynamically large system.

### C. Condition for adiabatic time evolution for special $\Delta$

At special values of  $\Delta$ , i.e.,  $\Delta = -\cos(\pi/p)$  ( $p = 2, 3, 4, \dots$ ), the adiabatic ground state energy  $\varepsilon_{\text{AGS}}(A)$  has an exceptionally long period  $\Delta A = 2\pi/(p-1)$  as discussed in Sec. II B. Our numerical results in Sec. III A suggest that, as long as the applied electric field  $E = 2\pi/T$  is sufficiently weak, the system follows the adiabatic ground state  $|\Psi_{\text{AGS}}(A)\rangle$  and exhibits a Bloch oscillation with temporal period  $T/(p-1)$  as demonstrated in Figs. 4(a)–4(c). Here we estimate the strength of the electric field required to observe this nontrivial oscillation.

We want to study the condition for adiabatic time evolution as done in the previous section for generic  $\Delta$ . However, this time the Landau-Zener formula is not directly applicable, since there are many level crossings in the many-body spectrum as shown in Fig. 2(b). Here we instead evaluate the overlap  $p_{\text{AGS}}(t) = |\langle \Psi_{\text{AGS}}(A(t)) | \Psi(t) \rangle|^2$  in Eq. (15) after a single period, i.e., at time  $t = T/(p-1)$ . As an example, we focus on the case of  $\Delta = -\cos(\pi/3) = -0.5$ .

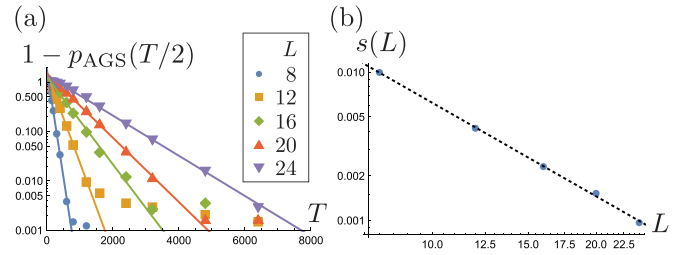


FIG. 6. (a)  $1 - p_{\text{AGS}}(t)$  at  $t = T/2$  for  $\Delta = 0.5$  ( $p = 3$ ) as a function of  $T = 2\pi/E$ . Fitting lines are obtained by using data within  $0.02 < 1 - p_{\text{AGS}}(t) < 0.7$ . (b) The slope of the fitting lines in (a) against the system size  $L$ . The dotted line represents the linear fitting  $s(L) = cL^{-2.096}$ .

Our numerical results are summarized in Fig. 6. We find that the probability of nonadiabatic transition behaves as

$$1 - p_{\text{AGS}}(T/2) \simeq \exp[-s(L)T] = \exp\left[-\frac{2\pi s(L)}{E}\right]. \quad (17)$$

The  $L$  dependence of the slope  $s(L)$  of the fitting line in Fig. 6(a) is plotted in Fig. 6(b). By further fitting, we find

$$s(L) \simeq cL^{-b}, \quad b = 2.096. \quad (18)$$

Combining these results, we see the condition for adiabatic transition:

$$E \ll 2\pi cL^{-b}. \quad (19)$$

Observe the formal similarity between our numerical results for  $\Delta = -0.5$  [Eqs. (17) and (19)] and those obtained by the Landau-Zener formula for generic  $\Delta$  [Eqs. (13) and (16)]. We also note that the power  $b$  in Eq. (19) (2.096 for  $\Delta = -0.5$ ) is much smaller than the power  $2a$  in Eq. (16) for generic  $\Delta$  [see Fig. 5(c)]. Therefore, although the electric field must be very small to realize the adiabatic process, the required smallness of the electric field is much relaxed for special values of  $\Delta$ .

### D. Bloch oscillations under a stronger field

The subtle differences caused by  $\Delta$  discussed above are irrelevant under a strong electric field. Indeed, we find qualitatively the same behavior regardless of the value of  $\Delta$  for the  $T = 1$  case as shown in Fig. 7. The corresponding electric field  $E = 2\pi$  is so strong that nonadiabatic transitions occur everywhere.

We also present the behavior of  $\varepsilon(t)$  and  $j(t)$  for  $T = 1, 10, 10^2, \dots, 10^6$  for comparison in Fig. 8. These plots imply that behaviors of the  $\varepsilon(t)$  and  $j(t)$  depend on the details of the system except for the two limiting cases of adiabatic and nonadiabatic transitions.

## IV. DISCUSSIONS

In this work we demonstrated that interacting electrons can in principle exhibit Bloch oscillations even under a weak electric field when the interaction is fine tuned. This is the case when the nonlinear Drude weights introduced in Ref. [7] remain finite in the large  $L$  limit to all orders of response. The expected behavior of the oscillations in the electric current density is similar to the noninteracting limit in the sense that

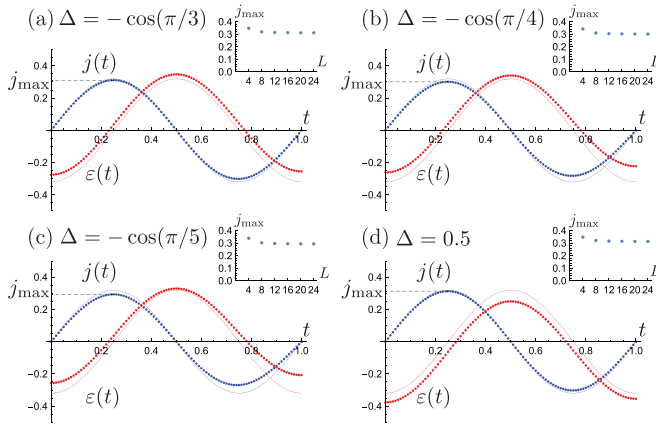


FIG. 7. Same as Fig. 4 but for  $T = 1$ , which corresponds to a strong electric field  $E = 2\pi$  in the unit of  $J/(ea)$ . Solid curves represent the analytic expressions for  $\Delta = 0$  for comparison (see the caption of Fig. 1).

the amplitude of the oscillation remains nonzero in the limit of large system size. Yet, there are also some differences, for example, in the number of peaks and the period of the oscillations for a given adiabatic process, as one can see by comparing Fig. 1(b) and Figs. 4(a)–4(c). In particular, the frequency of the oscillation becomes  $a(p-1)E/(2\pi)$  for  $\Delta = -\cos(\pi/p)$ .

When the interaction is not exactly at the fine-tuned value, the oscillation in the limit of the weak electric field is suppressed in a large but finite system [Fig. 4(d)]. However, even in that case, when the applied electric field is not weak enough, nonadiabatic transitions occur and one observes nontrivial oscillations of the electric current density, as shown in Fig. 7. In fact, our estimate based on the Landau-Zener formula in (16) suggests that the adiabatic limit is difficult to be realized in a thermodynamically large system. This, in turn, implies that pathological behaviors of nonlinear Drude weights observed in Refs. [7,10,11] do not come into play for a realistic strength of the applied electric field.

#### ACKNOWLEDGMENTS

We thank Kazuaki Takasan and Masaki Oshikawa for collaborations in previous related works. We thank Hosho Katsura for partially informing us of their on-going result based on the Bethe ansatz, which supports the finiteness of nonlinear Drude weights we numerically observed [35]. We also thank Masaki Oshikawa and Hosho Katsura for their valuable comments on the earlier version of the draft. The work of Y.F. is supported by JSPS KAKENHI Grant No. JP20K14402. The work of H.W. is supported by JSPS KAKENHI Grant No. JP20H01825 and by JST PRESTO Grant No. JPMJPR18LA.

#### APPENDIX A: ANALYTIC FORMULAS

Here we summarize the analytic expressions derived in previous studies. We parametrize  $\Delta$  as  $\Delta = \cos \gamma$  with

$0 \leq \gamma < \pi$ . The ground state energy density  $\bar{\epsilon}_{\text{GS}}$  and the linear Drude weight  $\bar{D}_1$  in the large  $L$  limit are given by [20,24]

$$\bar{\epsilon}_{\text{GS}} = \frac{1}{4} \cos \gamma - \frac{1}{2} \sin \gamma \int_{-\infty}^{\infty} dx \frac{\sinh[(\pi - \gamma)x]}{\sinh(\pi x) \cosh(\gamma x)}, \quad (\text{A1})$$

$$\bar{D}_1 = \frac{Kv}{\pi} = \frac{\pi}{4} \frac{\sin \gamma}{\gamma(\pi - \gamma)}. \quad (\text{A2})$$

In this work we obtain a new analytic expression for the maximum value of  $\epsilon_{\text{AGS}}(A)$  for  $\gamma = \pi - \pi/p$ :

$$\begin{aligned} \epsilon_{\text{AGS}}\left(\frac{\pi}{p-1}\right) &= \frac{1}{4} \cos \gamma + \frac{1}{2} \sin \gamma \\ &\times \int_{-\infty}^{\infty} d\omega \frac{\sinh[(\pi - \gamma)\omega] \tanh[(\pi - \gamma)\omega]}{\sinh(\pi\omega) \sinh(\gamma\omega)}. \end{aligned} \quad (\text{A3})$$

This is the same expression as the one in Eq. (5) in the main text. See Appendix B for the derivation.

The Luttinger parameter  $K$  and the velocity parameter  $v$  are given by [17,34]

$$K = \frac{\pi}{2(\pi - \gamma)}, \quad (\text{A4})$$

$$v = \frac{\pi \sin \gamma}{2\gamma}. \quad (\text{A5})$$

Higher-order Drude weights  $\bar{D}_3$  [7,10] and  $\bar{D}_5$  [10] are given by

$$\bar{D}_3 = -\frac{\sin \gamma}{16\gamma(\pi - \gamma)} \left( \frac{\Gamma(\frac{3\pi}{2\gamma})\Gamma(\frac{\pi-\gamma}{2\gamma})^3}{\Gamma(\frac{3(\pi-\gamma)}{2\gamma})\Gamma(\frac{\pi}{2\gamma})^3} + \frac{3\pi \tan(\frac{\pi^2}{2\gamma})}{\pi - \gamma} \right), \quad (\text{A6})$$

$$\begin{aligned} \bar{D}_5 &= \frac{3 \sin \gamma}{64\pi\gamma(\pi - \gamma)} \left( \frac{\Gamma(\frac{5\pi}{2\gamma})\Gamma(\frac{\pi-\gamma}{2\gamma})^5}{\Gamma(\frac{5(\pi-\gamma)}{2\gamma})\Gamma(\frac{\pi}{2\gamma})^5} \right. \\ &\quad - \frac{5\Gamma(\frac{3\pi}{2\gamma})^2\Gamma(\frac{\pi-\gamma}{2\gamma})^6}{3\Gamma(\frac{3(\pi-\gamma)}{2\gamma})^2\Gamma(\frac{\pi}{2\gamma})^6} + \frac{15\pi^2 \tan^2(\frac{\pi^2}{2\gamma})}{(\pi - \gamma)^2} \\ &\quad \left. + \frac{5\pi \tan(\frac{\pi^2}{2\gamma})}{\pi - \gamma} \frac{\Gamma(\frac{3\pi}{2\gamma})\Gamma(\frac{\pi-\gamma}{2\gamma})^3}{\Gamma(\frac{3(\pi-\gamma)}{2\gamma})\Gamma(\frac{\pi}{2\gamma})^3} \right). \end{aligned} \quad (\text{A7})$$

The formulas for  $\bar{D}_3$  and  $\bar{D}_5$  are finite when  $\pi/3 < \gamma < \pi$  and  $\pi/2 < \gamma < \pi$ , respectively.

The coefficient  $\lambda$  of the least irrelevant perturbation due to Umklapp scattering derived in Ref. [33] reads

$$\begin{aligned} \lambda &= \frac{4\Gamma(\beta^{-2})}{\Gamma(1 - \beta^{-2})} \left( \frac{\Gamma(1 + \frac{\beta^2}{2-2\beta^2})}{2\sqrt{\pi}\Gamma(1 + \frac{1}{2-2\beta^2})} \right)^{2/\beta^2-2} \\ &= \frac{4\Gamma(\frac{\pi}{\pi-\gamma})}{\Gamma(\frac{-\gamma}{\pi-\gamma})} \left( \frac{\Gamma(\frac{\pi+\gamma}{2\gamma})}{2\sqrt{\pi}\Gamma(\frac{\pi+2\gamma}{2\gamma})} \right)^{4K-2}, \end{aligned} \quad (\text{A8})$$

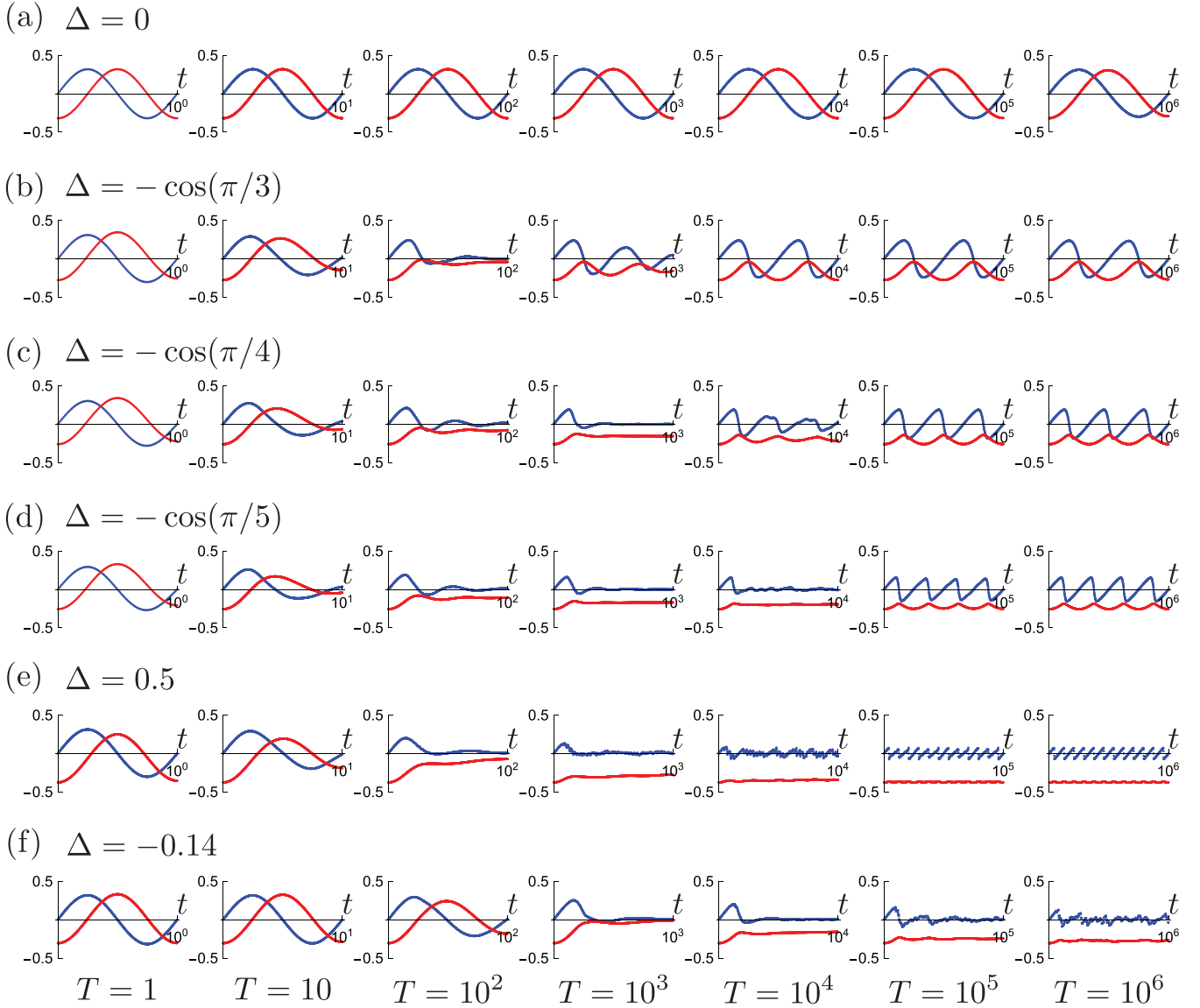


FIG. 8. The plot of the energy density  $\varepsilon(t)$  (red) and the current density  $j(t)$  (blue) under the electric field  $E = 2\pi/T$  for various values of  $T$  and  $\Delta$ :  $T = 1, 10, 10^2, \dots$ , and  $10^6$  and  $\Delta = 0, -\cos(\pi/3), -\cos(\pi/4), -\cos(\pi/5), 0.5$ , and  $-0.14$ . The system size is  $L = 24$ . While the gap above the adiabatic ground state is maximized at  $\Delta = -0.14$  for  $\Delta < 0$  and  $L = 24$ ,  $T = 10^6$  is not large enough to see  $O(L)$  oscillations as observed for  $\Delta = 0.5$ .

where  $\beta^2 = 1 - \gamma/\pi$ , which gives

$$\begin{aligned}
 C &= |\lambda| \frac{\pi \sin \gamma}{2\gamma} (2\pi)^{4K-1} \\
 &= 4\pi^2 \frac{\sin \gamma}{\gamma} \frac{\Gamma(\frac{\pi-\gamma}{\pi-\gamma})}{|\Gamma(\frac{-\gamma}{\pi-\gamma})|} \left( \sqrt{\pi} \frac{\Gamma(\frac{\pi+\gamma}{2\gamma})}{\Gamma(\frac{\pi+2\gamma}{2\gamma})} \right)^{4K-2}. \quad (\text{A9})
 \end{aligned}$$

#### APPENDIX B: DERIVATION OF Eq. (A3)

In this Appendix we present the analytic expressions regarding the energy density of the adiabatic ground state in the thermodynamic limit as a function of  $A \in [0, \Delta A/2]$ , where  $\Delta A = 2\pi/(p-1)$  and the range of  $A$  is halved from the evenness of the energy density function [36]. We consider the special values of  $\Delta$ , i.e.,  $\gamma = \pi - \pi/p$  ( $p = 3, 4, 5, \dots$ ).

By combining the Bethe ansatz and a generalized Wiener-Hopf technique [24,37–39] and taking care of the string excitations [40], the energy density of the adiabatic ground state in the thermodynamic limit as a function of  $A \in [0, \pi/(p-1)]$  is determined by the following integration:

$$\varepsilon_{\text{AGS}}(A) = \frac{1}{4} \cos \gamma - \sin \gamma \int_{B_R(A)}^{B_S(A)} dx' \rho(x', A) a(x'), \quad (\text{B1})$$

where  $a(x) = \sin \gamma / (\cosh x - \cos \gamma)$ .  $B_S(A)$ ,  $B_R(A)$ ,  $\rho(x, A)$  are the solutions of the system of equations:

$$\begin{aligned}
 a(x) &= 2\pi \rho(x, A) - \int_{B_R(A)}^{B_S(A)} dx' \rho(x', A) a(x-x'), \\
 &\text{for } x > \min[B_S(A), B_R(A)], \quad (\text{B2})
 \end{aligned}$$

$$\int_{B_R(A)}^{\infty} dx' \rho(x', A) = \frac{1}{2} - \frac{A}{\pi}, \quad (\text{B3})$$

$$\int_{B_S(A)}^{\infty} dx' \rho(x', A) = \frac{A}{2\pi}, \quad (\text{B4})$$

where  $\min S$  denotes the smallest element among  $S$ . Equation (B2) is the Bethe equation in the thermodynamic limit. Equations (B3) and (B4) reflect the conservation of the  $z$  component of the total spin. The behaviors of  $B_R(A)$  and  $B_S(A)$  are summarized as follows: as  $A \rightarrow +0$ , we have  $B_R(A) \rightarrow -\infty$  but  $B_S(A) \rightarrow \infty$ ; when  $A$  is increased in the interval  $(0, \Delta A/2)$ ,  $B_R(A)$  increases, whereas  $B_S(A)$  decreases; at  $A = \pi/p$ ,  $B_R(A) = B_S(A) = 0$ ; as  $A \rightarrow \pi/(p-1) - 0$ , we have  $B_R(A) \rightarrow \infty$  while  $B_S(A) \rightarrow -\infty$ .

The energy density is obtained explicitly at three special values of  $A$ . When  $A = 0$ , it reproduces Eq. (A1) [41]:

$$\begin{aligned} \varepsilon_{\text{AGS}}(0) = \bar{\varepsilon}_{\text{GS}} &= \frac{1}{4} \cos \gamma - \frac{1}{2} \sin \gamma \\ &\times \int_{-\infty}^{\infty} d\omega \frac{\sinh [(\pi - \gamma)\omega]}{\sinh(\pi\omega) \cosh(\gamma\omega)}. \end{aligned} \quad (\text{B5})$$

While for  $A = \pi/(p-1)$ , we obtain the maximum value of the energy density:

$$\begin{aligned} \varepsilon_{\text{AGS}}\left(\frac{\pi}{p-1}\right) &= \frac{1}{4} \cos \gamma + \frac{1}{2} \sin \gamma \\ &\times \int_{-\infty}^{\infty} d\omega \frac{\sinh^2 [(\pi - \gamma)\omega]}{\sinh(\pi\omega) \sinh(\gamma\omega) \cosh [(\pi - \gamma)\omega]}. \end{aligned} \quad (\text{B6})$$

The choice of dummy variable  $\omega$  above reminds us that the integration is done in the Fourier space of  $x$ . The energy density is the most easily expressed at  $A = \pi/p$ , where

$$\varepsilon_{\text{AGS}}\left(\frac{\pi}{p}\right) = \frac{1}{4} \cos \gamma. \quad (\text{B7})$$

- 
- [1] R. Resta, *J. Phys.: Condens. Matter* **30**, 414001 (2018).
- [2] J. Feldmann, K. Leo, J. Shah, D. A. B. Miller, J. E. Cunningham, T. Meier, G. von Plessen, A. Schulze, P. Thomas, and S. Schmitt-Rink, *Phys. Rev. B* **46**, 7252 (1992).
- [3] K. Leo, P. H. Bolivar, F. Brüggemann, R. Schwedler, and K. Köhler, *Solid State Commun.* **84**, 943 (1992).
- [4] C. Waschke, H. G. Roskos, R. Schwedler, K. Leo, H. Kurz, and K. Köhler, *Phys. Rev. Lett.* **70**, 3319 (1993).
- [5] T. Dekorsy, R. Ott, H. Kurz, and K. Köhler, *Phys. Rev. B* **51**, 17275 (1995).
- [6] We set  $e = \hbar = 1$  throughout this work. Also, our sign convention of  $A$  is opposite to the usual one.
- [7] H. Watanabe and M. Oshikawa, *Phys. Rev. B* **102**, 165137 (2020).
- [8] C. L. Kane and M. P. A. Fisher, *Phys. Rev. Lett.* **68**, 1220 (1992).
- [9] C. L. Kane and M. P. A. Fisher, *Phys. Rev. B* **46**, 15233 (1992).
- [10] Y. Tanikawa, K. Takasan, and H. Katsura, *Phys. Rev. B* **103**, L201120 (2021).
- [11] M. Fava, S. Biswas, S. Gopalakrishnan, R. Vasseur, and S. A. Parameswaran, *Proc. Natl. Acad. Sci.* **118**, e2106945118 (2021).
- [12] K. Takasan, M. Oshikawa, and H. Watanabe, [arXiv:2105.11378](https://arxiv.org/abs/2105.11378).
- [13] L. D. Landau, *Phys. Z. Sowjetunion* **2**, 19 (1932).
- [14] C. Zener and R. H. Fowler, *Proc. R. Soc. London Ser. A* **137**, 696 (1932).
- [15] C. Wittig, *J. Phys. Chem. B* **109**, 8428 (2005).
- [16] A. Bastianello and A. De Luca, *Phys. Rev. Lett.* **122**, 240606 (2019).
- [17] J. Sirker, *Int. J. Mod. Phys. B* **26**, 1244009 (2012).
- [18] M. Oshikawa, *Phys. Rev. Lett.* **84**, 1535 (2000).
- [19] F. C. Alcaraz, M. N. Barber, and M. T. Batchelor, *Ann. Phys.* **182**, 280 (1988).
- [20] B. Sutherland and B. S. Shastry, *Phys. Rev. Lett.* **65**, 1833 (1990).
- [21] T. Fukui and N. Kawakami, *J. Phys. Soc. Jpn.* **65**, 2824 (1996).
- [22] N. Yu and M. Fowler, *Phys. Rev. B* **46**, 14583 (1992).
- [23] There is a factor of 4 error in Ref. [22], which stated on page 14590 that the period of  $\Phi = AL$  is  $8\pi L/(p-1)$  for  $\Delta = \cos \mu = -\cos(\pi/p)$  with  $p = \pi/(\pi - \mu) \in \mathbb{N}$  in our notation and the sign convention of  $\Delta$ . Our formula  $\Delta A = 2\pi/(p-1)$  gives the correct period  $2\pi$  in the noninteracting case ( $p = 2$ ).
- [24] C. J. Hamer, G. R. W. Quispel, and M. T. Batchelor, *J. Phys. A: Math. Gen.* **20**, 5677 (1987).
- [25] M. Oshikawa, *Phys. Rev. Lett.* **90**, 236401 (2003).
- [26] M. Mierzejewski and P. Prelovšek, *Phys. Rev. Lett.* **105**, 186405 (2010).
- [27] T. Kato, *J. Phys. Soc. Jpn.* **5**, 435 (1950).
- [28] S. Bachmann, W. De Roeck, and M. Fraas, *Phys. Rev. Lett.* **119**, 060201 (2017).
- [29] T. Oka, R. Arita, and H. Aoki, *Phys. Rev. Lett.* **91**, 066406 (2003).
- [30] T. Oka, *Phys. Rev. B* **86**, 075148 (2012).
- [31] The Landau-Zener formula quoted in Eq. (3) of Ref. [29] missed a factor of 1/4 in the exponent.
- [32] R. A. Römer, H.-P. Eckle, and B. Sutherland, *Phys. Rev. B* **52**, 1656 (1995).
- [33] S. Lukyanov, *Nucl. Phys. B* **522**, 533 (1998).
- [34] T. Giamarchi, *Quantum Physics in One Dimension*, International Series of Monographs on Physics (Oxford University Press, New York, 2004).
- [35] Y. Tanikawa and H. Katsura, *Phys. Rev. B* **104**, 205116 (2021).
- [36] N. Byers and C. N. Yang, *Phys. Rev. Lett.* **7**, 46 (1961).
- [37] M. Takahashi, *Thermodynamics of One-Dimensional Solvable Models* (Cambridge University Press, Cambridge, 1999).
- [38] J. Sirker and M. Bortz, *J. Stat. Mech.: Theory Exp.* (2006) P01007.
- [39] P. Morse and H. Feshbach, *Methods of Theoretical Physics Bind I* (McGraw-Hill, New York, 1953).
- [40] H. Bergknoff and H. B. Thacker, *Phys. Rev. D* **19**, 3666 (1979).
- [41] C. N. Yang and C. P. Yang, *Phys. Rev.* **150**, 327 (1966).